



PERGAMON

Available online at www.sciencedirect.com

SCIENCE @ DIRECT®

Vision Research 43 (2003) 2315–2331

Vision
Research

www.elsevier.com/locate/visres

The role of local grouping and global orientation contrast in perception of orientation-modulated textures

Nicolaas Prins^{a,1}, Natasha K. Nottingham^a, Alexander J. Mussap^{a,*}

^a School of Psychology, Deakin University, 221 Burwood Highway, Burwood, Melbourne 3125, Australia

Received 1 May 2002; received in revised form 2 May 2003

Abstract

We explored the contribution to perception of orientation-modulated textures of visual processes selective either for orientation contrast or orientation grouping. To distinguish between these two processes we manipulated the axis of local grouping of texture elements independently of the direction of global orientation modulation. The general question posed was whether visibility of texture structure (measured as threshold for discriminating spatial-frequency of texture structure) is dependent on the magnitude of orientation contrast, strength and direction of local grouping, or some combination of the two. We demonstrated that the factor of primary importance is the amplitude of global orientation contrast rather than the presence of local grouping content. Using orientation-interleaved textures (containing two superimposed textures modulated around orthogonal orientations), we further showed that orientation single-opponent processes are a more likely candidate for detecting orientation contrast than double-opponent processes.

© 2003 Elsevier Ltd. All rights reserved.

Keywords: Texture perception; Orientation contrast; Perceptual grouping; Gabors; Spatial-frequency discrimination

1. Introduction

Psychophysical evidence suggests that the human visual system decomposes retinal images into their component orientations at particular spatial scales (e.g., Campbell & Robson, 1968). This is supported neurophysiologically by the existence of neurons of primate visual cortex that are conjointly sensitive to stimulus orientation and spatial frequency/size (Hubel & Wiesel, 1962). In line with this, computational models of pattern vision (e.g., Bovik, Clark, & Geisler, 1990; Malik & Perona, 1990) typically include a front-end array of linear spatial filters of narrow orientation and spatial-frequency selectivity designed to extract first-order structure; that is, structure defined by luminance.

Linear filtering of this sort cannot, however, account for the perception of second-order structure defined by

the modulation of first-order content. This requires the addition of a second stage of linear filtering that operates on the outputs of the first stage following the introduction of a non-linearity (usually modelled as response rectification; Chubb & Sperling, 1988). For example, detection of *contrast* modulations might be accomplished by second-stage filters selective for patterns of differential activity of first-stage inputs over space. This general approach is consistent with electrophysiological evidence of cells in areas 17 and 18 of cat visual cortex that are sensitive to second-order, contrast-defined structure (Zhou & Baker, 1993).

Since differential activity can be produced by modulation over space along any dimension for which particular filters are sensitive, it follows that the same two-stage process might account for the detection of second-order structure other than that which is defined by contrast, for example, texture boundaries formed by an abrupt change in *orientation* (e.g., Malik & Perona, 1990; Rubenstein & Sagi, 1993; Sutter, Beck, & Graham, 1989, 1995). A physiologically plausible candidate for such second-order processes are orientation *single-opponent* neurons with excitatory/inhibitory receptive areas tuned to a single orientation such that a maximal response

* Corresponding author. Tel.: +61-3-92517103; fax: +61-3-9244-6858/6852.

E-mail address: mussap@deakin.edu.au (A.J. Mussap).

¹ Present address: Department of Psychology, Peabody Building, University of Mississippi, University, MS 38677.

is given in response to a high contrast region of that orientation surrounded by either a low contrast region or a high contrast region of orthogonal orientation.

Ambiguity inherent in the responses of such processes (e.g., confusing orientation change with change in contrast or spatial frequency) can be resolved by modifying the way in which orientation information from the first stage is organised, for example, by having second-stage filters combine first-stage inputs in double-opponent fashion, that is, with two superimposed concentric receptive areas of orthogonal orientation selectivity and identical response polarity (e.g., vertical-ON and horizontal-OFF centre/vertical-OFF and horizontal-ON surround; see Gray & Regan, 1998; Kingdom & Keeble, 1996; Prins & Mussap, 2000; Rubenstein & Sagi, 1993; but see also Prins & Mussap, 2001 for criticism of explanations involving double-opponency). Neurons with orientation-opponent properties have been discovered in primate areas V1 and MT (Knierim & Van Essen, 1992; Olavarria, DeYoe, Knierim, Fox, & Van Essen, 1992; Sillito, Grieve, Jones, Culdeiro, & Davis, 1995; von der Heydt, Peterhans, & Dürsteler, 1992; Zipser, Lamme, & Schiller, 1996).

Psychophysical evidence points to the existence of an explicit code for the structure of orientation-modulated (OM) structure that is consistent with the operation of orientation-opponent processes: (i) sensitivity to periodic OMs is well-modelled by the operation of filters tuned to OM structure (Kingdom & Keeble, 1996; Kingdom, Keeble, & Moulden, 1995) and demonstrates bandpass tuning to OM spatial frequency (Gray & Regan, 1998), (ii) masking effects by luminance-modulated gratings on detection of OMs (Arsenault, Wilkinson, & Kingdom, 1999), as well as the perceived location of OMs with skewed orientation distributions (Prins & Mussap, 2000), are both dependent on envelope rather than carrier structure, and (iii) adapting to the location of OMs shifts the perceived location of subsequently presented OMs irrespective of the dissimilarity in orientation content between adapting and test OMs (Prins & Mussap, 2001).

The problem with orientation-opponency is that it predicts that the visibility of OMs should depend exclusively on OM amplitude. Contrary to this, detection thresholds for OM textures are influenced by the difference between the orientation around which the modulation is centred (the “base” orientation) and the axis of the modulation itself (Kingdom et al., 1995). Given that OMs with different “base” orientations differ in their appearance primarily in terms of the curvature of perceptual chains formed between adjacent texture elements, it follows that a likely candidate for explaining this effect is local grouping processes, perhaps through the operation of local cooperative interactions between neurons akin to those thought to extract curved paths (e.g., “association fields”; Field, Hayes, & Hess, 1993), or through the activity of second-stage neurons that extract locally

straight paths by combining outputs from collinearly oriented first-stage neurons (e.g., “collator/collector” mechanisms; Morgan & Hotopf, 1989; Moulden, 1994).

There is ample psychophysical (Beck, Prazdny, & Rosenfeld, 1983, 1987; Field et al., 1993; Grossberg & Mingolla, 1985; Morgan & Hotopf, 1989; Moulden, 1994; Mussap & Levi, 1996, 1997; Nothdurft, 1992; Polat & Sagi, 1993, 1994; Smits, Vos, & van Oeffelen, 1985; Tripathy, Mussap, & Barlow, 1999) and neurophysiological (Mitchison & Crick, 1982; Rockland & Lund, 1983; Schmidt, Goebel, Lowel, & Singer, 1997) evidence for grouping mechanisms such as these, and preferences for particular axes of grouping offer a simple explanation and test of the effects of base orientation on OM visibility. For example, it has been shown that grouping is superior when the elements are oriented parallel to the local curved path rather than perpendicular to it (Field et al., 1993) and that positional jitter is most detrimental when it is perpendicular to the path rather than parallel to it (Tripathy et al., 1999). These preferences suggest the following predictions regarding the influence of local grouping processes on OM perception: First, as reported previously (Kingdom et al., 1995), OM perception should be superior when grouping occurs along the axis of OM modulation, particularly when the elements to be grouped are oriented around this orientation rather than being orthogonal to it; second, grouping along the axis orthogonal to the OM axis should disrupt detection of OMs, particularly when the elements are oriented along paths that are orthogonal to the OM axis.

Examples of OM-base combinations are provided in Fig. 1. In these textures, all with identical OM amplitude and global spatial frequency, it is apparent that perceived OM structure is influenced by the strength and direction of local grouping chains between texture elements. The aim of the present series of experiments was to quantify and explore this effect and to distinguish it from contributions to OM perception from putative orientation-opponent processes. Our approach was to constrain the placement and orientation of individual elements within OM textures such that local groupings would be parallel or orthogonal to the direction of orientation modulation (always horizontal), and to vary base orientation such that these groupings were either parallel or orthogonal to the orientation of local texture elements (Fig. 1 provides examples). We could then obtain modulation amplitude thresholds for *discriminating* some property of OM structure (in our experiments, OM spatial frequency) for combinations of base orientation and axis of grouping.

In the first experiment we replicate Kingdom et al.’s (1995) observation that OM textures with horizontal base orientation (i.e., where base orientation is parallel to the axis of orientation modulation) are more salient than those where these dimensions are orthogonal. However, we fail to demonstrate that these effects are related to the direction and strength of local grouping. In subsequent

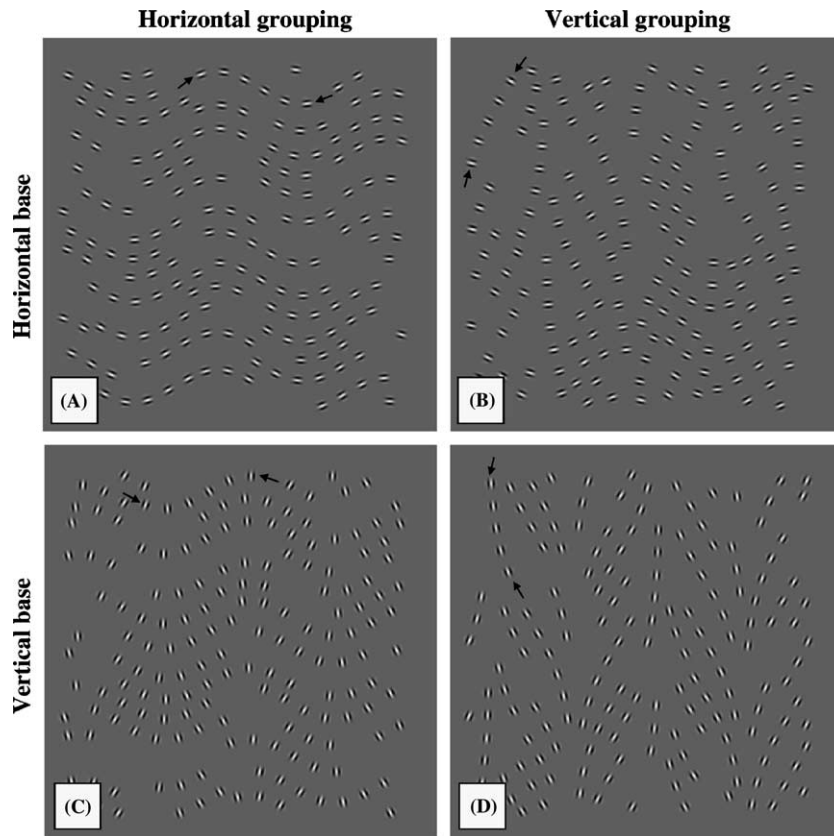


Fig. 1. Examples of OM textures produced by combination of one base orientation (horizontal or vertical): (A) Base(H)/grouping(H), (B) Base(H)/grouping(V), (C) Base(V)/grouping(H), and (D) Base(V)/grouping(V). The modulations are along the horizontal axis and are of high spatial-frequency. Arrows point to examples of grouping chains.

experiments we demonstrate that discriminability of OMs is unaffected by positional disarray of texture elements, but is severely disrupted by orientation-and-position disarray. This is inconsistent with the involvement of grouping processes but is consistent with orientation-opponency. Subsequent experiments using *interleaved* pairs of OMs with orthogonal base orientations reveal that single-, rather than double-opponency, is the most feasible candidate. Taken together, these results suggest the following explanation of the superior visibility of OM textures in which base orientation is parallel to the direction of orientation modulation: (i) the excitatory and inhibitory regions of orientation single-opponent processes are arranged along an axis that is either parallel or perpendicular to their orientation preference (rather than being concentric centre-surround), and (ii) in the human visual system there is a predominance of the parallel-arrangement type (see Fig. 11).

2. General methods

2.1. Participants

Participants were the authors (P1 [N.N.], P2 [A.M.], and P3 [N.P.]) and four practiced naive participants.

2.2. Apparatus

All stimuli were presented on a 21" EIZO high-resolution monochrome monitor at a distance of 1.5 m, gamma corrected to 32,000 grey levels (from 0 to 55 cdm^{-2}) via a Visionworks™ calibration system. These stimuli were generated by a Cambridge Research Systems™ CRS2/3F graphics card which was controlled by custom-written C-programs based on Visionworks™ graphics routines.

2.3. Stimuli

2.3.1. Texture elements

Stimuli were 2-D textures that occupied a region that was $8.3^\circ \times 8.3^\circ$ and of mean luminance (27.5 cdm^{-2}). The textures differed in terms of the location and shape of the 170 elements that filled the texture region. In Experiments 1 to 3 these elements were oriented Gabors (see Fig. 1 for examples), created by multiplying a 2-D cosine carrier wave of spatial frequency $f = 7.21 \text{ cpd}$, amplitude $A = 25.5 \text{ cdm}^{-2}$, and orientation ($0^\circ \leq \theta \leq 179^\circ$, clockwise from vertical) with a symmetric 2-D Gaussian envelope of standard deviation $\sigma = 0.069^\circ$:

$$G(x, y) = A \cos(2\pi fs) \exp\left(-\frac{x^2 + y^2}{2\sigma^2}\right),$$

where $s = x \cos(\theta) + y \sin(\theta)$.

In Experiment 4 the texture elements were non-oriented, circular Gabors (refer to Fig. 8), created by multiplying a *circular* cosine carrier wave of spatial frequency $f = 7.21$ cpd, and amplitude $A = 25.5$ cdm⁻², by the same symmetric 2-D Gaussian envelope as used for the oriented Gabors, according to the following formula:

$$G(x, y) = A \cos(2\pi fr) \exp\left(-\frac{x^2 + y^2}{2\sigma^2}\right),$$

where $r = (x^2 + y^2)^{0.5}$.

2.3.2. Orientation-modulated textures: Base orientation and axis of grouping

In Experiments 1, 2, and 3, stimuli were OM textures created by periodic and smooth modulation of the orientation of Gabor elements along the horizontal plane (according to the method detailed in Appendix A). The orientation around which the modulation was centred (the “base” orientation) was either parallel (horizontal) or perpendicular (vertical) to the direction of modulation. In a departure from previous research using OM textures (cf. Kingdom et al., 1995), Experiments 1 to 3 also constrained the *placement* of the Gabors in order to control the axis along which the Gabors could form grouped “chains”. For these textures grouping was constrained to be either parallel (horizontal) or perpendicular (vertical) to the direction of orientation modulation. It is important to stress that irrespective of which axis of grouping was employed to determine Gabor placement, the orientation of these Gabors was determined exclusively by their position along the x -axis such as not to violate the shape (phase and amplitude) of the sinusoidal distribution that defined the orientation modulation.

Textures were composed of arrangements of grouping chains each containing either three or six aligned Gabors with a distance of 0.55° , measured along the grouping chain, between the centres of consecutive Gabors. Ninety to ninety five of the Gabors were placed in chains composed of six Gabors; these chains were randomly positioned in the display one by one under the constraint of both Gabor orientation (as described above) with the distance between centres of Gabors from different chains set to be larger than 0.37° . Gabors that extended over the edge of the screen were removed and did not count towards the 90–95 total. The remaining Gabors were placed in chains composed of three Gabors and randomly positioned under the constraints just mentioned.

By manipulating base orientation and axis of grouping four basic types of OM texture were created (depicted in Fig. 1):

- (i) Base(H)/grouping(H): horizontal base orientation and horizontal axis of grouping;
- (ii) Base(H)/grouping(V): horizontal base orientation and vertical axis of grouping;
- (iii) Base(V)/grouping(H): vertical base orientation and horizontal axis of grouping;
- (iv) Base(V)/grouping(V): vertical base orientation and vertical axis of grouping.

Pairs of these textures were orthogonal along three dimensions: base orientation relative to direction of orientation modulation (parallel in i and ii; perpendicular in iii and iv); axis of grouping relative to direction of orientation modulation (parallel in i and iii; perpendicular in ii and iv); base orientation relative to axis of grouping (parallel in i and iv; perpendicular in ii and iii).

For the non-oriented textures of Experiment 4, base orientation and, consequently, the relationship between base orientation and both direction of modulation and direction of grouping, were meaningless. Only the relationship between axis of grouping and direction of modulation was relevant. In all respects, the construction of grouping chains for these textures was identical to that described for the oriented textures except that the Gabors themselves were not oriented.

2.4. Procedure

OM textures of a single basic type were presented in blocks of 150 trials for 375 ms per trial. In half of these trials the orientation modulations were of “low” spatial-frequency (0.16 cpd) while in the other half they were of “high” spatial-frequency (0.24 cpd), with random order of presentation. The phase of the orientation modulation was entirely random from trial to trial.

The dependent variable in all experiments was the amplitude of orientation modulation, which varied between 1° and 30° . A 2-alternative forced-choice procedure was employed, in which the subject’s task was to indicate, after each trial, whether the texture was of low or high modulation spatial-frequency.² They accomplished this by a button press (left = low, right = high)

² We chose OM *spatial frequency discrimination* over the more obvious (and more frequently used) OM detection due to the difficulty in finding an appropriate standard in the latter case. Typically, researchers have required their subjects to decide between an OM at low amplitude and a non-OM texture (of the same amplitude but with all its elements positionally scrambled). Consider, however, that the non-OM, unlike its OM counterpart, has far greater local orientation contrast (the OM texture is a gradient in which local orientation differences are minimised). That is, subjects in such detection tasks could be responding on the basis of a salient visual cue (amount of local orientation contrast) that has little to do with the perception of global orientation-defined structure.

on a computer mouse. Immediately following the response, auditory feedback was provided (1 beep = low, 2 beeps = high) to facilitate learning the discrimination and to reinforce accurate responding.

At the beginning of the testing session, subjects became familiarised with both low and high spatial-frequency textures by use of a self-administered viewing procedure, whereby sample textures of either frequency were selected and displayed without time restrictions. The four types of texture were introduced in the order in which they would be tested. This was followed by an intensive training session in which blocks of trials were self-initiated and interrupted after about 50 trials, this was continued until both the subject felt confident with the discrimination task for that particular texture and the intermediate scores indicated that performance had reached asymptotic levels. The testing session followed, with at least 2 blocks and continued until scores stabilised.

After instructions and practice, testing of subjects proceeded, with the amplitude of OM corresponding to 75% correct responses determined by an adaptive maximum-likelihood procedure (the *Best PEST*; Pentland, 1980). The *Best PEST* used in the experiments employed three independent, randomly interleaved adaptive staircases of 50 trials each, with the initial OM amplitude randomised.

3. Experiment 1: The effects of base orientation and axis of grouping

To explore the role of local grouping processes on perception of OM textures the base orientation and axis of grouping of these textures were manipulated independently, and the effects of these manipulations measured in terms of changes to amplitude threshold for discriminating the spatial-frequency of modulation of the textures. It was hypothesised that a contribution from grouping processes would manifest itself in lower thresholds for textures in which the axis of grouping is parallel to the direction of orientation modulation (e.g., Fig. 1A and C), and higher thresholds for textures in which the axis of grouping is perpendicular to the direction of orientation modulation (i.e., Fig. 1B and D). Moreover, given evidence in the grouping literature that strength of grouping is greater when base orientation is parallel rather than perpendicular to the axis of grouping (Field et al., 1993), an interaction effect was predicted in which the effects of grouping (either facilitative or disruptive) are more pronounced when base orientation and axis of grouping are parallel (Fig. 1A and D) rather than perpendicular (Fig. 1B and C).

The four basic OM textures described in the Section 2 (and illustrated in Fig. 1) served as stimuli. These were: Base(H)/grouping(H); Base(H)/grouping(V); Base(V)/

grouping(H); and Base(V)/grouping(V). Procedures were as described in the Section 2.

3.1. Results and discussion

Preliminary data screening was conducted on amplitude thresholds. Since the *Best PEST* method is sensitive to accidental incorrect responses to high-amplitude (“easy”) textures, subjects’ individual data were first screened for outliers, defined as thresholds greater than 1.5 standard deviations from the mean, which were subsequently removed. Mean amplitude thresholds and ± 1 standard errors were calculated for each subject for each of the four textures, and plotted in Fig. 2.

A 2×2 within-subjects ANOVA was conducted for *Base Orientation* (two levels: horizontal and vertical) by *Axis of Grouping* (two levels: horizontal and vertical) which revealed only a significant main effect of base orientation ($F_{(1,6)} = 13.861, p < 0.05$). Inspection of Fig. 2 shows that six of the seven subjects produced lower

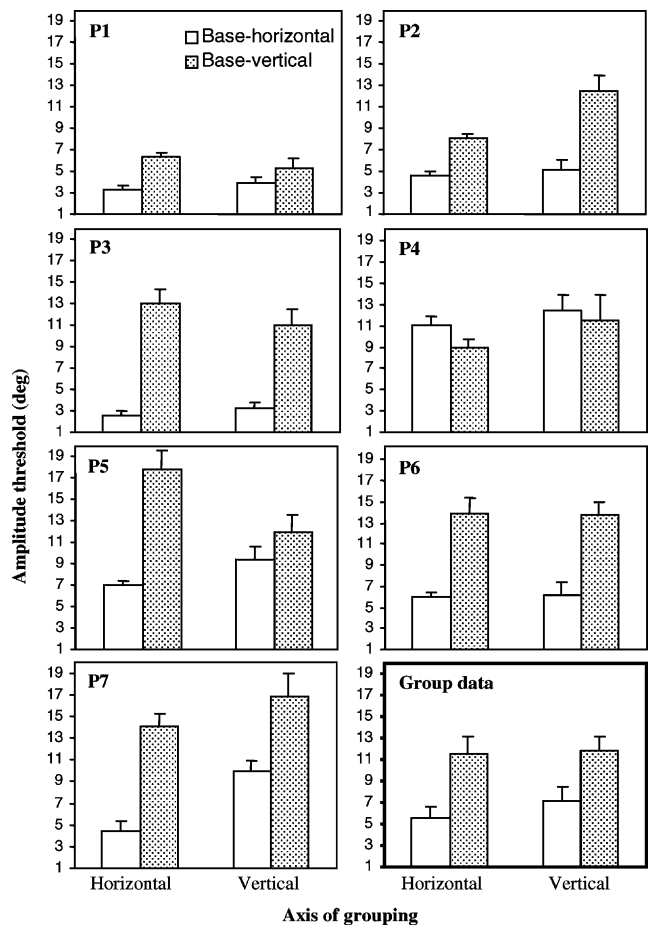


Fig. 2. Results of Experiment 1A: OM amplitude thresholds ($^{\circ}$) as a function of base orientation and axis of grouping. Group data (and corresponding error bars) are shown bottom right. ± 1 standard error bars are included for comparison.

thresholds for horizontal-base textures than for vertical-base textures. Neither the main effect of axis of grouping, nor the interaction between the two variables, were found to be significant.

As reported previously (Kingdom et al., 1995), base orientation was found to influence discriminability of orientation-modulation textures. However, the failure to find effects of axis of grouping or an interaction between axis of grouping and base orientation undermines the explanation of this effect based on local grouping processes. However, since our textures contained dense arrangements of elements it is possible that grouping effects *were* involved, but did not manifest themselves in changes in threshold levels simply because the method employed to produce grouping along one axis did not adequately prevent *accidental* groupings along the orthogonal axis (the texture in Fig. 1B is an excellent illustration of this). This interpretation is consistent with the pattern of responses given by subjects, in which greater *variability* in thresholds was evident with textures in which either intentional, or salient *unintentional*

axes of grouping (i.e., where base orientation is parallel to axis of grouping) were orthogonal to direction of orientation modulation. This is particularly evident with the Base(V)/grouping(H) texture (Fig. 1C) in which the grouping along the intended axis (horizontal) is weak compared to grouping along the unintended axis (vertical). For such textures, subjects would have two independent sources of grouping information (aside from the orientation modulation itself) from which to base their responses.

This interpretation was tested in a 2×2 (base orientation by axis of grouping) within-subjects ANOVA on *standard errors* of responses. The ANOVA revealed a main effect of base orientation, with standard errors for horizontal bases being significantly smaller than those for vertical bases ($F_{(1,6)} = 26.729, p < 0.005$), as well as a main effect of axis of grouping, with standard errors for horizontal axes being significantly smaller than those for vertical axes ($F_{(1,6)} = 13.864, p < 0.050$; see Fig. 3 for individual and group standard errors).

In the following experiment this “unintentional grouping” explanation was investigated by systematically disrupting the grouping chains contained in each of the four basic texture types and measuring tolerance to this disruption.

4. Experiment 2: The effects of position and orientation perturbation

Two forms of texture perturbation were employed to estimate the sensitivity to local position and orientation of visual processes mediating perception of OM textures. With the first form of perturbation, *position disarray* (PD), Gabors were randomly removed from their local grouping chains, replaced in a random location within the texture region, and their orientation in the new position made consistent with the global OM function (see Fig. 4A). The disruptive effect of element position on perceptual grouping is well documented (e.g., Beck, Rosenfeld, & Ivry, 1989; Moulden, 1994; Tripathy et al., 1999), and this method of perturbation was designed to quantify the importance of intact grouping chains and, therefore, the contribution of grouping mechanisms to texture perception. With the second form of perturbation, *orientation-and-position disarray* (OPD), Gabors were randomly removed from their local grouping chains and randomly replaced, but in this case they retained their original orientation such that their new orientation did no longer necessarily agree with the global OM function (see Fig. 4B). This condition (particularly when compared to the PD manipulation) was designed to quantify the importance of visual processes that integrate orientation information globally (e.g., processes of global orientation-oppo-

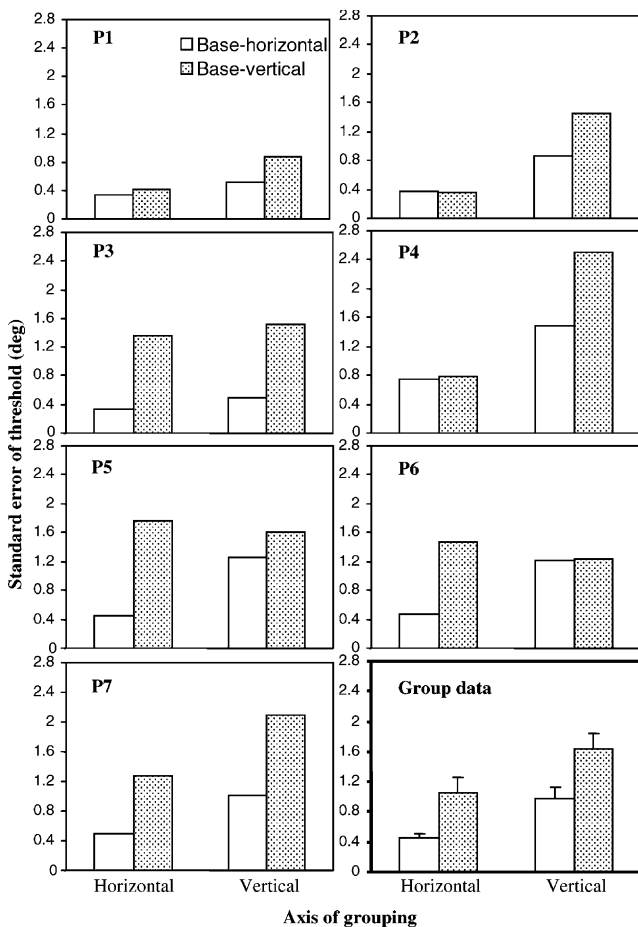


Fig. 3. Results of Experiment 1B: Standard errors of thresholds ($^{\circ}$) as a function of base orientation and axis of grouping. Group data (and corresponding error bars) are shown bottom right. ± 1 standard error bars are included for comparison.

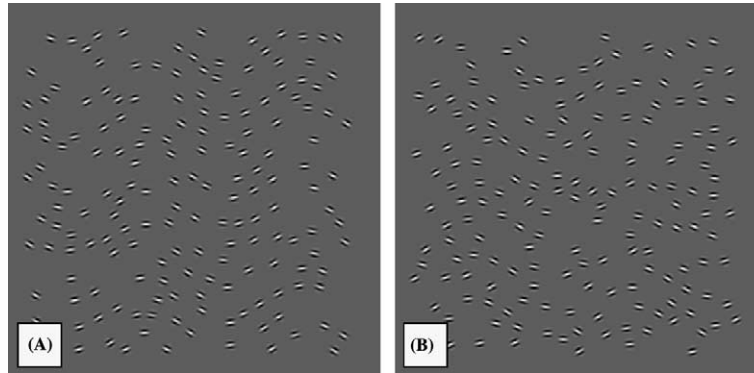


Fig. 4. Examples of (A) 50% position-disarray (PD) and (B) 50% orientation-and-position-disarray (OPD) applied to a high spatial-frequency OM of horizontal base orientation and horizontal direction of modulation.

The effects of PD and OPD were quantified by application of *intrinsic noise* fits (Barlow, 1956; Pelli, 1990), the rationale being that texture element perturbation should affect OM spatial-frequency discrimination thresholds noticeably only when the extent of stimulus perturbation (quantified as % texture elements perturbed) equals or exceeds the intrinsic noise of underlying visual processes.

Intrinsic noise estimates derived from PD would be a direct measure of the degree to which grouping-type visual processes undersample texture elements *exclusively* from locations within grouping chains (this undersampling could take the form of stunted grouping processes, of grouping processes with a sparse input array, or some combination of both). We were confident that grouping-type processes could be singled out in this way because, by replacing the texture elements removed during PD at orientations appropriate for their new random location, both the overall density of texture elements as well as the global distribution of orientation would remain constant as %PD increased. If grouping processes do not limit OM thresholds (i.e., if the underlying processes integrate orientation over space but not necessarily within grouping chains), then the effects of PD would *not* take the form of intrinsic noise functions.

Intrinsic noise estimates derived from OPD would reveal the level of undersampling within visual processes that integrate orientation samples irrespective of their local position within grouping chains. Furthermore, since texture elements were removed and then replaced in new locations such that their orientation was inconsistent with the global OM function, the effects of OPD would also be a measure of the orientation uncertainty of these processes. While both of these effects of OPD would, in theory, include (and be confounded with) those associated with grouping-type processes, it is important to note that since we found *no* effects of PD (see results below for more details), intrinsic noise estimates associated with OPD could be interpreted *exclusively* as

orientation uncertainty in *non*-grouping-type visual processes.

Aside from ascertaining whether the processes underlying OM perception are of a grouping- or non-grouping type, we were also interested in deriving estimates of intrinsic noise for the purpose of identifying the involvement of the same visual process under diverse stimulus conditions. For our purposes, therefore, it did not matter whether intrinsic noise reflected undersampling and/or orientation uncertainty, but whether or not the value of intrinsic noise remained constant or changed as base orientation and axis of grouping were manipulated, thereby indicating whether or not the same or different visual processes are involved (this was particularly useful in testing for the involvement of these processes in subsequent experiments).

The four basic textures were employed (see Section 2) in combination with the two modes of stimulus perturbation (PD and OPD). The number of Gabors perturbed in each block was between 0 to 68 (0–40%). For both types of perturbation, the Gabors were randomly repositioned such that their distance from centres of neighbouring Gabors was larger than 0.37° . Procedures were as described in the Section 2. The addition of type of perturbation (PD and OPD), and level of perturbation (0, 3, 5, 10, 15, 20, 30, and 40% of Gabors) to base orientation (2 levels) and axis of grouping (2 levels) made a total of 64 stimulus conditions, each tested in separate blocks of 150 trials. For each block, level of perturbation was constant across trials, and its presentation order was randomised.

4.1. Results and discussion

For each subject in each condition, intrinsic noise functions were fit to means of OM thresholds for the eight levels of OPD. Intrinsic noise fits were of the following form:

$$\text{Threshold} = k\sqrt{\sigma_c^2 + \sigma_i^2}$$

where threshold corresponds to orientation-modulation amplitude, k is a constant, σ_e^2 is the extrinsic noise level (measured in % Gabors undergoing OPD), and σ_i^2 is the intrinsic noise level (reported in *effective* % of OPD) which corresponds to the OPD level that causes thresholds to increase by a factor of $\sqrt{2}$. Means of thresholds for the eight levels of PD did not correspond to intrinsic noise functions and were thus fit with a linear function. As noted in Section 4 this suggests that the effects of OPD could be interpreted as intrinsic uncertainty in processes that are not involved in integrating orientation along grouping chains.

Inspection of the data (Fig. 5A and B) shows that thresholds for baseline (no perturbation), and low levels of either form of perturbation, were lower for horizontal-base textures than vertical-base textures, confirming the results of the previous experiment. However, for levels of perturbation greater than 16%, the two forms of perturbation differed markedly. With PD no effect

was observed, suggesting that the position of individual Gabors in grouping chains is irrelevant to processes of texture perception. This is not consistent with a role for perceptual grouping processes.

However, for the three subjects, OPD was shown to have a detrimental effect on performance. Making the texture task more difficult, by increasing OPD, resulted in higher overall thresholds for the vertical-base textures, which raised their functions on the y -axis, but did not result in systematic variations for intrinsic noise levels compared to those of the horizontal-base textures. Intrinsic noise values are displayed in the graphs (Fig. 5), the sample means range from $M = 18.36$, $S.D. = 0.20$ for Base(H)/grouping(V) to $M = 21.70$, $S.D. = 4.73$ for Base(V)/grouping(H).

The pattern of results obtained strongly suggests that a single class of mechanism is operating in all of the four basic texture types, and that this mechanism is sensitive to global orientation change over space as would be the orientation-opponent processes described in Section 1.

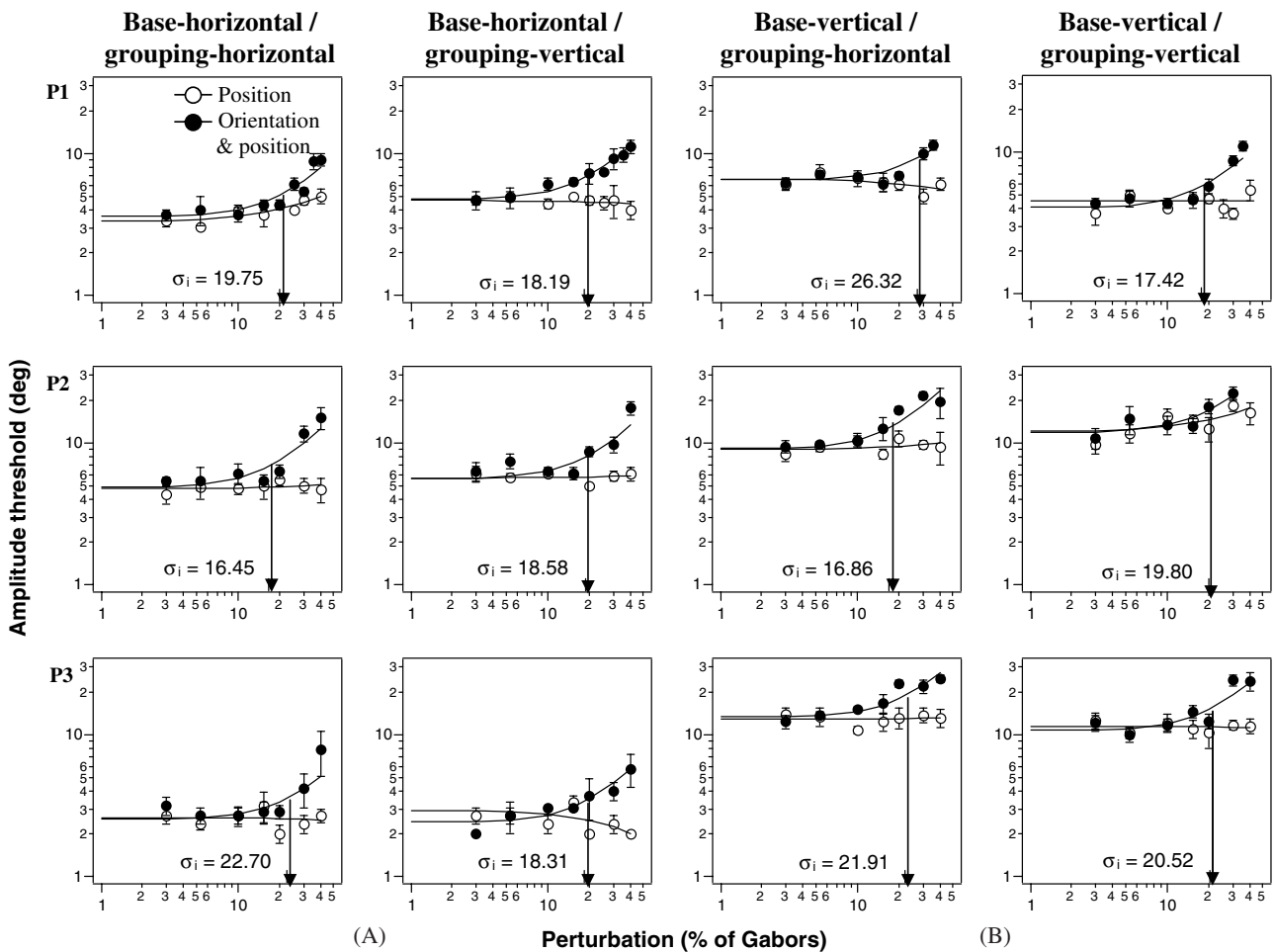


Fig. 5. Results of Experiment 2: OM amplitude thresholds ($^{\circ}$) as a function of base orientation, axis of grouping, percent PD, and percent OPD. PD data are fit with linear functions, while OPD data are fit with intrinsic noise functions. Arrows point to estimates of intrinsic noise values. ± 1 standard error bars are included for comparison.

5. Experiment 3: The effects of interleaved horizontal-base and vertical-base modulations

To explore the role of orientation-opponency in texture perception, textures were constructed that should not be detectable to orientation double-opponent processes. This was achieved by randomly interleaving pairs of OM textures with orthogonal base orientations (see Fig. 6). The rationale was that such textures would conjointly stimulate centre and surround regions of double-opponent processes, resulting in zero net excitation. In addition, it was reasoned that if grouping processes are indeed involved, but that their sensitivity is simply inferior to that of orientation-opponent processes, then precluding orientation-opponent mechanisms from contributing to thresholds should reveal the contribution from grouping processes (i.e., interleaved textures with a horizontal axis of grouping should be more easily discriminated than interleaved textures with a vertical axis of grouping).

For each texture, 50% of the Gabors had horizontal base orientations and 50% had vertical base orientations. Grouping chains were placed on the screen in the same manner as Experiment 1 but order of placement alternated between chains of horizontal Gabors and chains of vertical Gabors. This resulted in two texture types:

- (i) Base(H + V)/grouping(H)—horizontal base orientation and horizontal axis of grouping interleaved

with vertical base orientation and horizontal axis of grouping.

- (ii) Base(H + V)/grouping(V)—horizontal base orientation and vertical axis of grouping interleaved with vertical base orientation and vertical axis of grouping.

These two texture types were administered with eight levels of PD (0%, 3%, 5%, 10%, 15%, 20%, 30%, and 40%), which created 16 stimulus conditions.

5.1. Results and discussion

For each subject for each texture type, a linear fit was applied to the means of the eight levels of PD (as with all previous PD data; see Fig. 7). Mean thresholds for the three subjects for both interleaved textures indicate that they could discriminate these textures as well as non-interleaved types. This precludes a role for orientation double-opponent processes in discrimination of OM textures at threshold. Furthermore, for both interleaved texture types, mean thresholds with zero perturbation were comparable and performance did not deteriorate with increased PD up to 40% (indeed, all three subjects could perform the OM discrimination at comparable amplitudes even with PDs of 100%). As with the results of the previous experiment, this is inconsistent with the involvement of grouping processes (at least at threshold levels of OM amplitude).

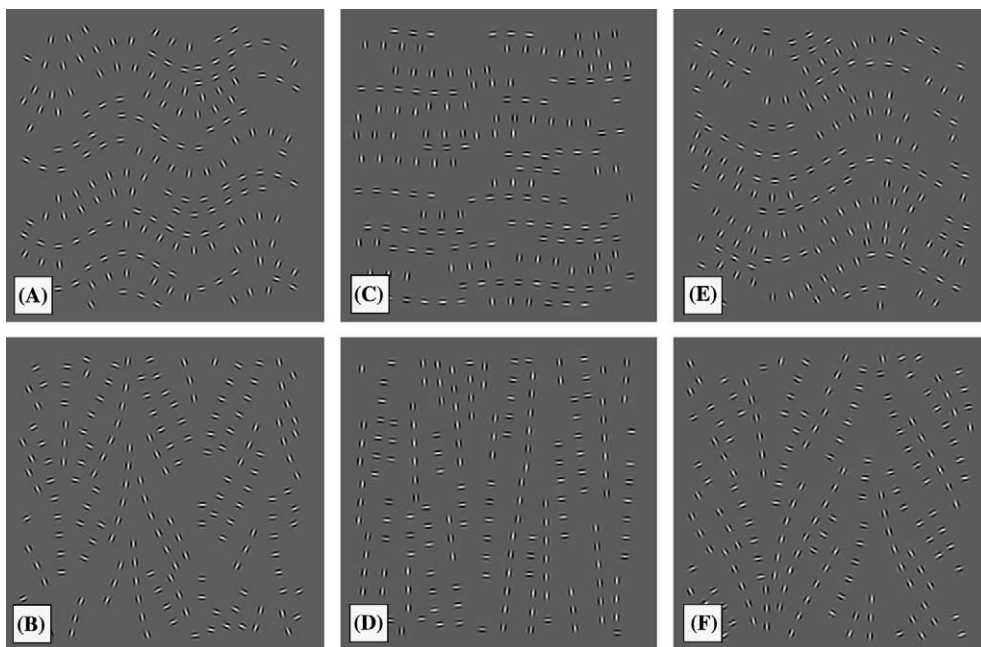


Fig. 6. Examples of orientation-interleaved textures of Experiment 3. (A) Horizontal axis of grouping; (B) vertical axis of grouping, with both OMs of high spatial-frequency and at a modulation amplitude around five times threshold (30°). (C) Horizontal axis of grouping; (D) vertical axis of grouping, again both of high spatial-frequency but this time at a modulation amplitude at around threshold (6°). (E) Horizontal axis of grouping; (F) vertical axis of grouping, with both OMs of low spatial-frequency and high amplitude (30°).

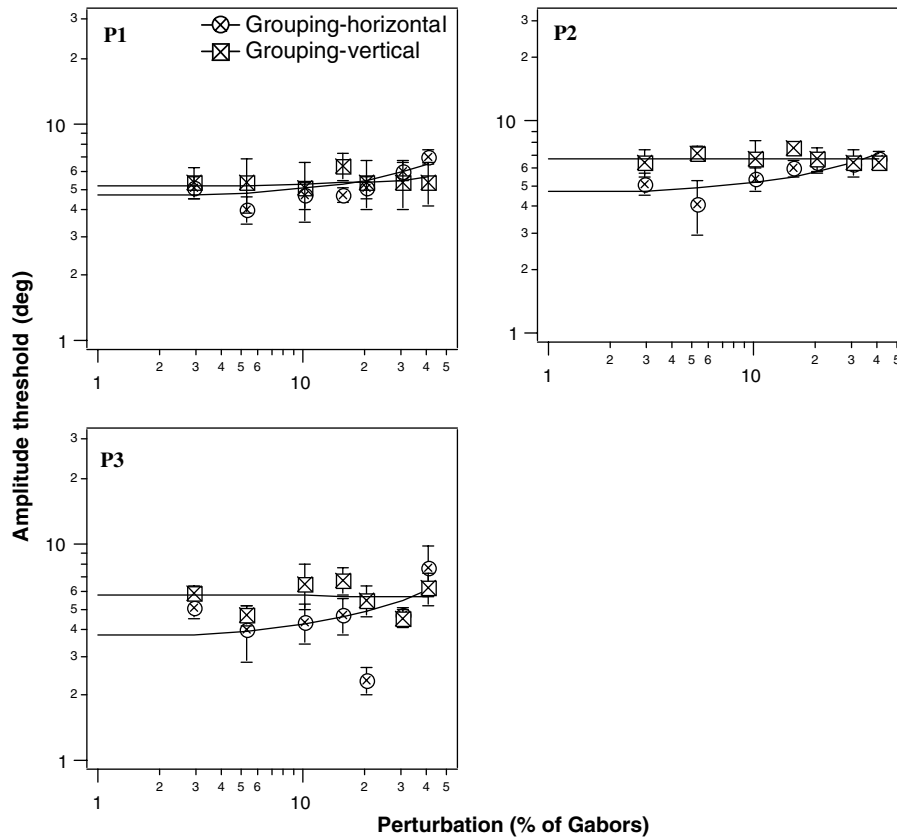


Fig. 7. Results of Experiment 3: Amplitude thresholds ($^{\circ}$) for orientation-interleaved OMs as a function of axis of grouping and percent PD. PD data are fit with linear functions. ± 1 standard error bars are included for comparison.

An anonymous reviewer has suggested that certain hypothetical double-opponent mechanisms might be able to respond to our OM textures (e.g., Graham, Sutter, & Venkatesan, 1993). For example, consider a neuron with a horizontally elongated (e.g., Gabor-shaped) double-opponent receptive field consisting of a horizontal-ON/vertical-OFF center and horizontal-OFF/vertical-ON sidelobes. Such a neuron would be activated by our textures if its (H+/V-) center was positioned on a string of Gabor micropatterns modulated around horizontal and its (H-/V+) sidelobes were positioned on strings of Gabor micropatterns modulated around vertical. Maximal responses from such a neuron would occur in regions where local texture orientation is close to the primary axes (i.e., at the zero point of the OM function), with reduced responses obtained in regions where local texture orientation is furthest from the primary axes (i.e., at the peak and trough of the OM function). However, there are several reasons that make it unlikely that such a neuron would limit OM perception at threshold amplitudes. First, the activation of such a neuron would be highly dependent on the exact positioning of its receptive field relative to the strings. With textures that are modulated along the horizontal axis (such as our OMs), even small shifts in the *vertical*

position of strings would be detrimental. Indeed, the reduction in the neuron's response due to small vertical shifts would be far greater than that which would occur along the horizontal axis in response to the OM itself. More importantly, such a neuron would only be able to signal the presence of orientation contrast, not the presence of orientation modulation, thus necessitating the involvement of *third-order* mechanisms that operate at a larger spatial scale.

6. Experiment 4: The effects of non-oriented texture elements

The irrelevance of both texture element positional perturbation and direction of grouping argues against a contribution from grouping processes. In Experiment 4, we explore this idea further by measuring sensitivity to spatially modulated textures composed of isotropic Gabors (see Fig. 8A and B). This would preclude the involvement of orientation-opponent processes as well as local *orientation-specific* grouping processes. Only grouping processes sensitive to Gabor position and spacing could be used to successfully extract and discriminate the structure of the modulation. Textures were

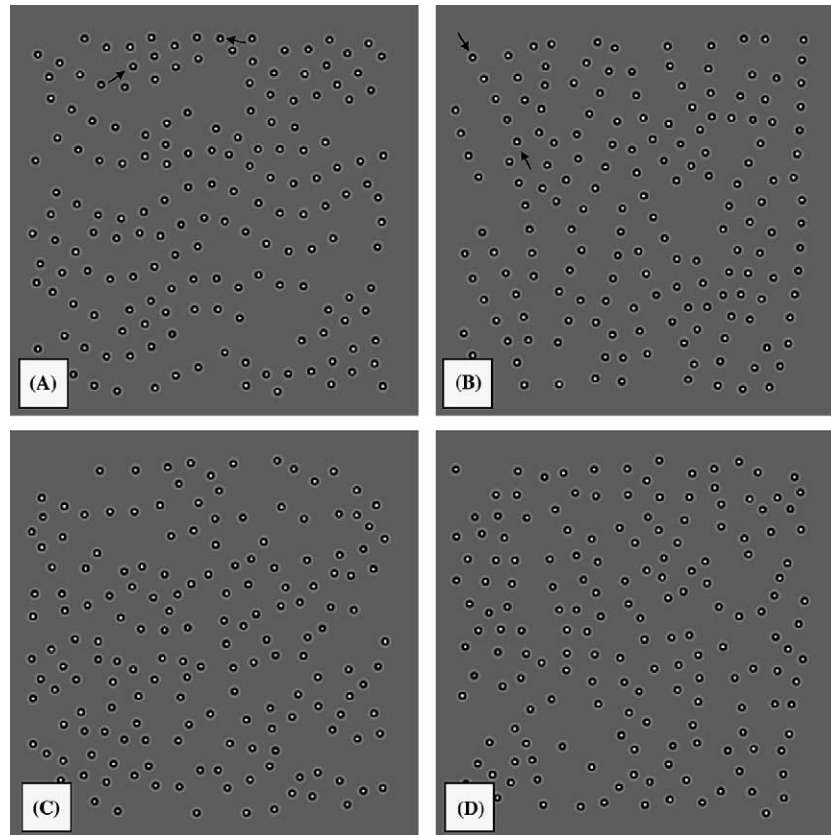


Fig. 8. Examples of non-oriented textures employed in Experiment 4. (A) Horizontal axis of grouping (0% PD), (B) vertical axis of grouping (0% PD), (C) Horizontal axis of grouping (50% PD), (D) vertical axis of grouping (50% PD). Arrows point to examples of six-element grouping chains.

constructed as described in the Section 2 with circular instead of oriented Gabors. This resulted in two texture types:

- (i) Base(circular)/grouping(H)—non-oriented base and horizontal axis of grouping.
- (ii) Base(circular)/grouping(V)—non-oriented base and vertical axis of grouping.

These textures were manipulated according to the positional-disarray method of Experiment 2 (see Fig. 8C and D). The two texture types were administered with positional disarray at eight levels of perturbation (0%, 3%, 5%, 10%, 15%, 20%, 30%, and 40%), which created 16 stimulus conditions that were presented to subjects in separate blocks after the method of Experiment 3.

The general predictions tested were (i) that the global structure of the non-oriented textures would be detectable and discriminable by subjects (this prediction is confirmed by inspection of the stimulus examples in Fig. 8), (ii) that global spatial-frequency discrimination thresholds would be higher than those obtained with oriented textures, and (iii) that different intrinsic noise estimates would be obtained relative to those of previous experiments, reflecting the involvement of different processes.

6.1. Results and discussion

Inspection of Fig. 9 shows that mean modulation amplitude thresholds for the non-oriented textures ($M = 5.67$, $S.D. = 1.89$ for base(circular)/grouping(H); $M = 11.58$, $S.D. = 4.32$ for base(circular)/grouping(V)) were higher than thresholds obtained with *spatially equivalent* oriented textures (e.g., Base(H)/grouping(H) from Experiments 1 and 2). More importantly, intrinsic noise estimates also differed markedly from those obtained with oriented textures ($M = 10.57$, $S.D. = 1.03$ for Base(circular)/grouping(H) versus $M = 18.36$, $S.D. = 0.20$ for Base(H)/grouping(V)). There was no overlap in the range of intrinsic noise values between the non-oriented base textures and the oriented-base textures.

The results suggest that although spatial structure in the form of local grouping chains can provide sufficient information with which to discriminate the spatial frequency of the structure, one's ability to do this is inferior to one's ability to discriminate the spatial structure of orientation-defined textures. Moreover, as suggested by the differences in intrinsic noise estimates, the underlying mechanisms involved in the two types of texture (oriented versus non-oriented) are unlikely to be the same.

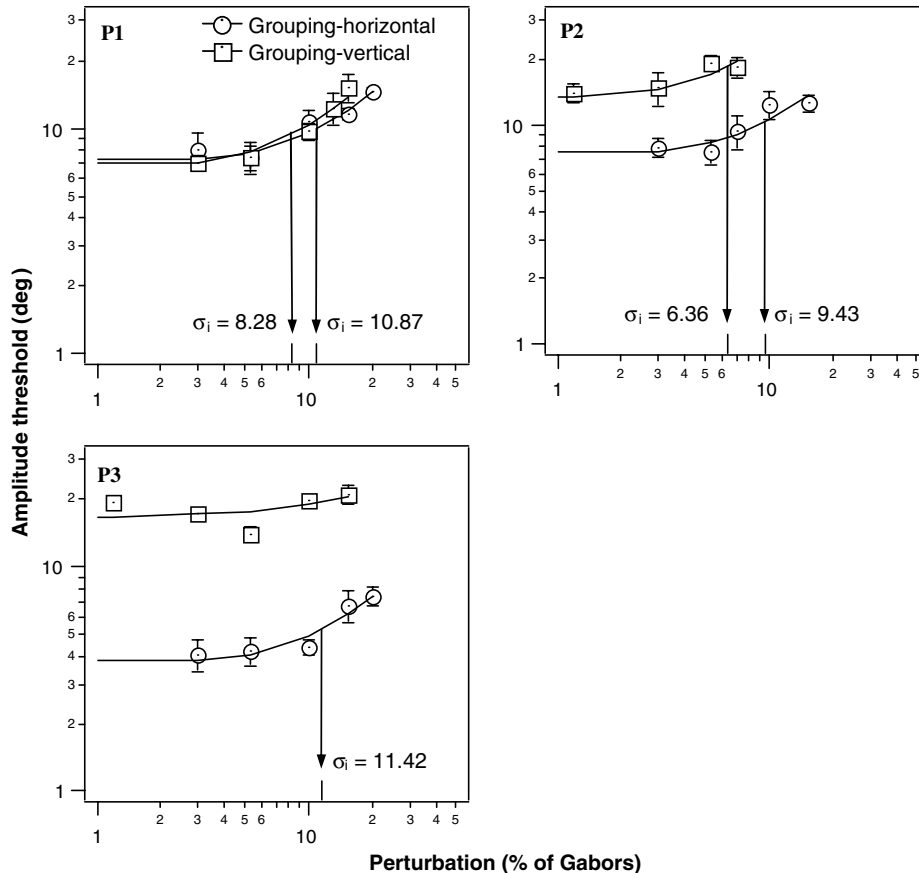


Fig. 9. Results of Experiment 4: Amplitude thresholds ($^{\circ}$) for non-oriented textures as a function of axis of grouping and percent PD. PD data are fit with intrinsic noise functions and arrows point to estimates of intrinsic noise values. ± 1 standard error bars are included for comparison.

7. General discussion

We explored the influence of grouping and orientation contrast on perception of OM structure by manipulating the axis of alignment of texture elements independently of the direction of orientation modulation and measuring resultant OM-frequency discrimination thresholds. In Experiment 1 we demonstrated that OM discrimination is superior when the direction of modulation is parallel to the orientation around which the modulation occurs. This replicates the finding of Kingdom et al. (1995) (in the context of OM discrimination rather than detection). The axis of local grouping (parallel versus perpendicular to direction of OM) was found to have no effects on thresholds. The role of grouping was investigated further in Experiment 2 in which it was shown that while positional perturbation of texture elements had no effect on performance, perturbation of position *and* orientation did elevate thresholds substantially. As with the results of Experiment 1, this suggests that it is the magnitude of global orientation contrast rather than the presence of local grouping that limits performance. This interpretation was bolstered by the findings that: (i) unchanging levels of intrinsic

(neural) noise were estimated for each axis of grouping condition, indicative of a *single* underlying neural mechanism irrespective of grouping content, and (ii) thresholds obtained when only grouping information was available (i.e., when circular-element textures were employed [Experiment 4]) were not only much higher but exhibited different intrinsic noise levels, indicative of the operation of a *different* type of neural mechanism.

Experiment 3 explored whether orientation double-opponent processes are involved in OM perception. The approach adopted was to employ horizontal-base textures interleaved with vertical-base textures, where the grouping direction of the two was the same. Such textures should be invisible to orientation double-opponent processes but accessible to single-opponent processes. Thresholds were almost as good as those for the non-interleaved textures of the previous experiments. This was taken as evidence against the involvement of double-opponent processes, a conclusion supported recently by Prins and Mussap (2001) using an adaptation technique. This conclusion is, however, at odds with recent reports that interleaved OMs, where the two OM components are in antiphase and possess identical base orientations (horizontal), are *difficult* to detect (King-

dom & Keeble, 2000). These authors argued that both single- and double-opponent processes (with their excitatory regions tuned to the shared base orientation of the OM components) should respond as well to such interleaved OMs as they do to single OMs, and hence rejected the involvement of orientation-opponent processes altogether.

Critical to Kingdom and Keeble's (2000) argument was their assumption that the orientation-opponent processes involved in the detection of their single- and dual-modulation textures received their front-end input from luminance filters tuned to the center orientation contained in the textures. This assumption, however, has since been undermined by Prins and Kingdom's (2002) discovery that low-amplitude OMs are instead detected by mechanisms tuned to orientations well outside the nominal orientation content of the OM. Prins and Kingdom (2002) argue that this is so because orientation-opponent processes respond to the *difference* in spectral orientation content between different texture regions.

To illustrate, in Fig. 10A are plotted the spectral contents across orientation at the peak (top graph) and the trough (middle graph) of a single-component OM texture. The distribution of spectral content across orientations is modelled here as Gaussian. The depth of modulation in the figure equals 5° which corresponds roughly to the thresholds we observed. The orientation bandwidth of the textures corresponds to the orientation bandwidth of our textures. In the bottom graph, where we plot the difference between the spectral content at the peak and the trough of the modulation, it can be seen that the mechanisms most responsive to this OM will have first-order filters tuned to about 20° either side of horizontal. In Fig. 10B are plotted the spectral contents of an interleaved counter-phase dual-modulation texture (such as those used by Kingdom & Keeble, 2000) at the two extremes in the modulation. In the top graph the texture's orientation content is plotted at the position

along the modulation where both components are horizontal. In the middle graph are plotted the orientation contents of the two components at the location in the modulation where one of the components is at its peak and the other component is at its trough, along with the sum of the two components. In the bottom graph we plot again the difference between the spectral content at the two extremes of the modulation. It is clear from the figure that such counter-phase dual-modulation textures contain much less 'orientation-opponent energy' that is available for an orientation-opponent process compared to a single-modulation texture. This is simply because the orientation content of the OM hardly varies along the modulation. The higher detection thresholds for Kingdom and Keeble's dual-modulation textures are thus not at all at odds with an explanation of their results in terms of an orientation-opponent process.

Finally, in Fig. 10C, we plot the orientation content of an interleaved texture where the two components are orthogonal and in-phase (such as those used in our Experiment 3) at the peak of the modulation (top graph) and the trough of the modulation (middle graph). In the bottom graph we again plot the difference between the spectral content at the peak and that at the trough of the modulation. From the bottom graph we can see that our interleaved modulation will lead to activation in four mechanisms, one pair tuned to about 20° either side from horizontal (the base orientation of one of the components), and another pair tuned to about 20° either side of vertical (the base orientation of the orthogonal component). Because each of these four mechanisms is responsive to only one of the two orthogonal OM components (each represented by half of the Gabors in the OM), the energy available to each of them will, of course, only be about half of the energy available to a mechanism processing a single-component OM. However, the *total* energy in the dual-component texture, summed across the four peaks in the 'difference distribution', will equal that of a single-component OM.

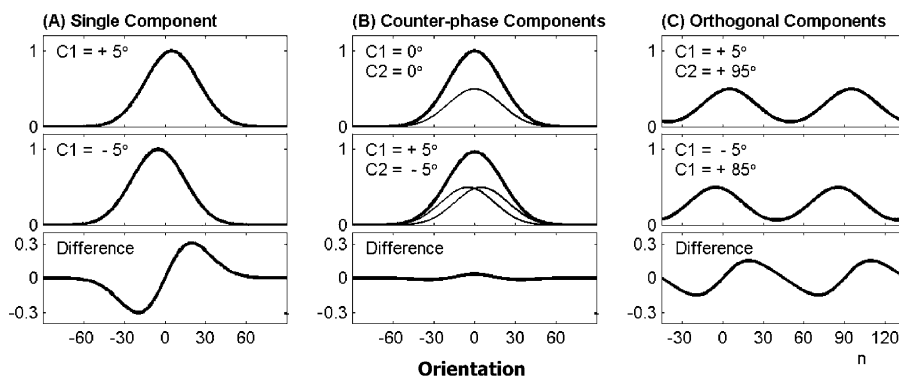


Fig. 10. Schematic illustration of the spectral content across orientation of (A) a single-component OM texture (B) a dual-component OM texture where the two components are in antiphase and share their base orientation (C) a dual-component OM texture where the two textures are in phase and orthogonal. The top and middle rows show the spectral content at two extremes along the modulation. The bottom row shows the difference in spectral content between two extremes along the modulation. (C1 = orientation of component 1, C2 = orientation of component 2).

Before considering the types of neural mechanisms that are consistent with our results, it is worth considering a possible confound noted by an anonymous reviewer of our manuscript. It is apparent from inspection of our OM stimuli that grouping chains are more salient when direction of grouping is parallel to base orientation (i.e., where alignment is ‘end-to-end’ rather than ‘side-to-side’). Similar effects have been reported in the perceptual grouping literature (e.g., Field et al., 1993). Could this confound between direction of grouping and base orientation have affected our results, and if so should this effect have been controlled?

Our response to this is that our results suggest no interaction between direction of grouping and base orientation. In Experiment 1 we found that OM thresholds were lower when base orientation was parallel to the direction of orientation modulation, irrespective of the direction of grouping. In Experiment 2 we found that OM thresholds were unchanged when individual Gabors were systematically removed from grouping chains (Fig. 5 [open circles]). This makes it highly unlikely that the perception of grouping chains is relevant to OM perception at threshold. Our results are instead consistent with interaction between base orientation and OM direction (see later in this section for a physiologically plausible explanation). Clearly, the relative salience of grouping across different conditions is not a relevant consideration at threshold levels of orientation modulation.

The original motivation for the research was to explain the effects of base orientation on OM visibility. Our expectation that this effect was related to direction

of grouping was not supported. How can we explain our results, including the lack of involvement of grouping processes at threshold, on the basis of the known response properties of neurons? Li and Li (1994) identified neurons in area V1 of cats with orientation single-opponent receptive field properties. That is, these neurons possessed central receptive-field regions sensitive (either excitatory or inhibitory) to one orientation, and a surround region of opposite sensitivity to the *same* orientation. Moreover, the surround regions of these neurons were usually found to be asymmetrical around the central region, with the strongest responses elicited from either side of the axis parallel to the orientation tuning of the central region (this is depicted in Fig. 11). These single-opponent neurons would thus be expected to be not only insensitive to local position and alignment of texture elements (as found in Experiment 2), but also exhibit greater sensitivity to orientation modulations that are in the direction parallel to base orientation (as found in Experiments 1 and 2).

To summarize, we have demonstrated that orientation-defined shape is detected primarily by mechanisms that are sensitive to differences in orientation content across space. These orientation contrast detectors are of the simplest possible configuration in that they possess a preference for a single orientation; that is, they are single-opponent rather than double-opponent for orientation. Interestingly, local grouping structure, while obviously salient and perceptually informative at suprathreshold levels of orientation contrast, does not account for the appearance of orientation-defined structure at threshold levels of orientation contrast.

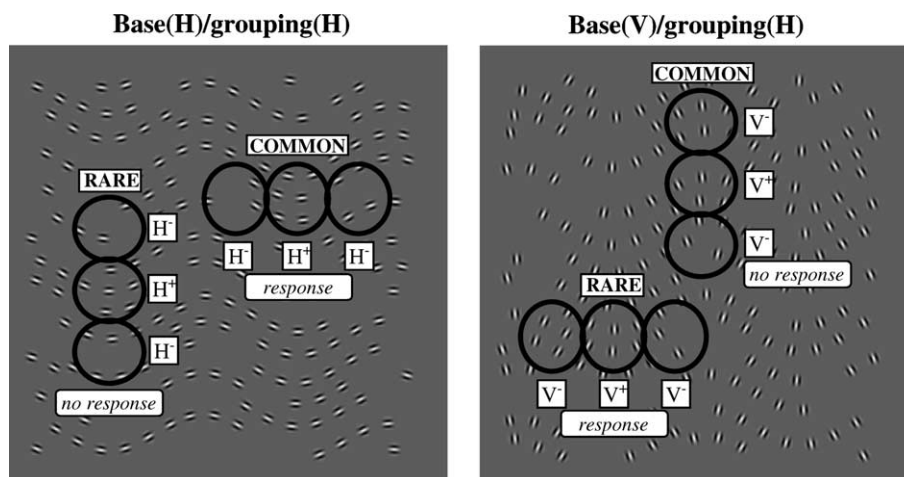


Fig. 11. Illustration of a possible explanation for the perceptual advantage associated with detecting and discriminating OM textures whose base orientation is parallel to the axis of modulation. Two examples of horizontally modulated OMs are provided: the left with a horizontal base; the right with a vertical base, and the receptive fields of two versions of orientation single-opponent neurons selective for base orientation are shown. Since both OMs are modulated in the horizontal direction, only opponent neurons that integrate along the horizontal axis will generate a response to the texture. However, physiological evidence points to a greater prevalence of orientation-opponent neurons that integrate along the axis of their orientation-selectivity (Li & Li, 1994). It follows, therefore, that neurons that are most active in the example will be those with a horizontal orientation-selectivity, coupled with a horizontal integration axis, and only in response to the horizontal-base texture on the left (i.e., the Base(H)/grouping(H) texture).

Grouping structure, especially as determined by the separation between texture elements, limits texture perception only when orientation information is absent or ambiguous. In conclusion, our results suggest that although both global orientation contrast and local grouping may contribute to perception of orientation-defined form, it is mechanisms sensitive to the former source of information that are more sensitive.

Acknowledgements

This research was supported by a grant from the Australian Research Council.

Appendix A

In those conditions where orientation was modulated around an average orientation of horizontal (i.e., where base orientation was horizontal; e.g., Fig. 1A and B), the orientation of Gabors was modulated as a function of horizontal position x (in degrees) as:

$$\theta(x) = \tan^{-1}[\tan(a \cdot \pi/180) \cdot \cos(2\pi fx)], \quad (\text{A.1})$$

(see Fig. 12, bottom panel) where amplitude a varied between 1° and 30° and modulation frequency f is either 0.16 or 0.24 cpd. The choice of this function, rather than a simple sinusoid, [i.e., $\theta(x) = a \cdot \sin(2\pi fx)$], was motivated by its mathematical convenience. Specifically, modulating orientation according to (A.1) results in convenient expressions (i.e., integratable) for the slopes

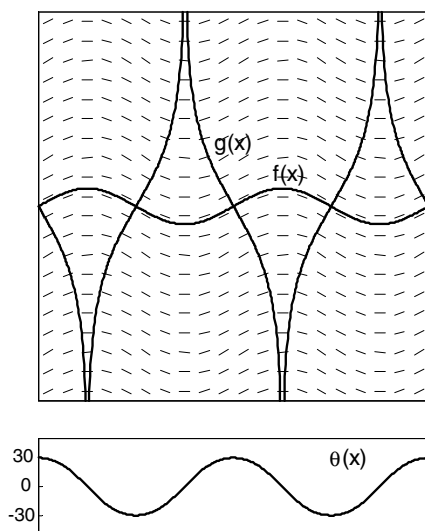


Fig. 12. Illustration of the orientation-modulation function $\theta(x)$, where amplitude $a = 30^\circ$ (bottom panel), the horizontal grouping curve $f(x)$ and the vertical grouping curve $g(x)$, (top panel). The short lines in the top panel have orientations corresponding to $\theta(x)$.

of (i) the function whose curve is parallel to orientation $\theta(x)$ at all x , and (ii) the function whose curve is perpendicular to orientation $\theta(x)$ at all x . Function (A.1) has the same amplitude as, and is highly correlated with (at least within the range of amplitudes used here, $r > 0.999$ for all amplitudes used), the simple sinusoid $\theta(x) = (a \cdot \pi/180) \cdot \cos(2\pi fx)$.

Horizontal grouping chains of Gabors should lie on a curve $y = f(x)$ which has a slope dy/dx which is parallel to $\theta(x)$, the orientation of the Gabors, i.e.

$$\begin{aligned} dy/dx &= \tan(\theta[x]) \Rightarrow dy/dx \\ &= \tan(\tan^{-1}[\tan(a \cdot \pi/180) \cdot \cos(2\pi fx)]) \\ &\Rightarrow dy/dx = \tan(a \cdot \pi/180) \cos(2\pi fx). \end{aligned} \quad (\text{A.2})$$

The function $f(x)$ is found by integration of (A.2):

$$\begin{aligned} f(x) &= \int \tan(a \cdot \pi/180) \cdot \cos(2\pi fx) dx \\ &\Rightarrow f(x) = [\tan(a \cdot \pi/180)/(2\pi f)] \cdot \sin(2\pi fx) + C. \end{aligned}$$

Given a point (x_0, y_0) on this function [$y_0 = f(x_0)$]

$$\begin{aligned} y_0 &= f(x_0) = [\tan(a \cdot \pi/180)/(2\pi f)] \cdot \sin(2\pi fx_0) + C \\ &\Rightarrow C = y_0 - [\tan(a \cdot \pi/180)/(2\pi f)] \cdot \sin(2\pi fx_0). \end{aligned}$$

Hence,

$$\begin{aligned} f(x) &= [\tan(a \cdot \pi/180)/(2\pi f)] \cdot [\sin(2\pi fx) - \sin(2\pi fx_0)] \\ &\quad + y_0. \end{aligned}$$

An instance of the curve $y = f(x)$ is displayed in Fig. 12. An example texture corresponding to this condition is shown in Fig. 1A.

Vertical grouping chains of Gabors, on the other hand, should lie on a curve $y = g(x)$ which has a slope dy/dx which is perpendicular to $\theta(x)$, the orientation of the Gabors, i.e.

$$\begin{aligned} dy/dx &= -1/[\tan(a \cdot \pi/180) \cdot \cos(2\pi fx)] \\ &\Rightarrow dy/dx = -\sec(2\pi fx)/\tan(a \cdot \pi/180), \\ &\quad \{2\pi fx \neq \pi/2 \pm k^* \pi; k = 0, 1, 2, \dots\}. \end{aligned} \quad (\text{A.3})$$

The function $g(x)$ is found by integration of (A.3):

$$\begin{aligned} g(x) &= \int -\sec(2\pi fx)/\tan(a \cdot \pi/180) dx \\ &\Rightarrow g(x) = -\ln |\sec(2\pi fx) \\ &\quad + \tan(2\pi fx)|/(2\pi f \cdot \tan[a \cdot \pi/180]) + C, \\ &\quad \{2\pi fx \neq \pi/2 \pm k^* \pi; k = 0, 1, 2, \dots\}. \end{aligned}$$

Given a point (x_0, y_0) on this function [$y_0 = g(x_0)$]

$$\begin{aligned} y_0 &= g(x_0) \\ &= -\ln |\sec(2\pi fx_0) + \tan(2\pi fx_0)|/(2\pi f \cdot \tan[a \cdot \pi/180]) \\ &\quad + C \Rightarrow C \\ &= y_0 + \ln |\sec(2\pi fx_0) \\ &\quad + \tan(2\pi fx_0)|/(2\pi f \cdot \tan[a \cdot \pi/180]). \end{aligned}$$

Hence,

$$g(x) = \{\ln |\sec(2\pi fx_0) + \tan(2\pi fx_0)| - \ln |\sec(2\pi fx) + \tan(2\pi fx)|\} / (2\pi f \cdot \tan[a \cdot \pi/180]) + y_0, \\ \{2\pi fx \neq \pi/2 \pm k^* \pi; k = 0, 1, 2, \dots\}.$$

An instance of the curve $y = g(x)$ is displayed in Fig. 12. An example texture corresponding to this condition is shown in Fig. 1B.

In those conditions where orientation was modulated around vertical (i.e., where base orientation was vertical; e.g., Fig. 1C and D) the orientation of Gabors was modulated as a function of horizontal position x (in degrees) as:

$$\theta(x) = \tan^{-1}[\tan(a \cdot \pi/180) \cdot \cos(2\pi fx)] + 90,$$

which is identical to formula (A.1) except that all orientations are rotated by 90° . Hence, in this case the curve $f(x)$ is orthogonal to the orientation of the Gabors (e.g., Fig. 1C) and the curve $g(x)$ is parallel to the orientation of the gabors (e.g., Fig. 1D).

References

- Arsenault, A. S., Wilkinson, F., & Kingdom, F. A. A. (1999). Modulation frequency and orientation tuning of second-order texture mechanisms. *Journal of the Optical Society of America A*, *16*, 427–435.
- Barlow, H. B. (1956). Retinal noise and absolute threshold. *Journal of the Optical Society of America*, *46*, 634–639.
- Beck, J., Prazdny, K., & Rosenfeld, A. (1983). A theory of textural segmentation. In J. Beck, B. Hope, & A. Rosenfeld (Eds.), *Human and machine vision* (pp. 1–38). New York: Academic Press.
- Beck, J., Rosenfeld, A., & Ivry, R. (1989). Line segregation. *Spatial Vision*, *4*, 75–101.
- Beck, J., Sutter, A., & Ivry, R. (1987). Spatial frequency channels and perceptual grouping in texture segregation. *Computer Vision, Graphics, and Image Processing*, *37*, 299–325.
- Bovik, A. C., Clark, M., & Geisler, W. S. (1990). Multichannel texture analysis using localized spatial filters. *IEEE Transactions on Pattern Analysis and Machine Intelligence*, *12*, 55–73.
- Campbell, F. W., & Robson, J. G. (1968). Application of fourier analysis to the visibility of gratings. *The Journal of Physiology*, *197*, 551–566.
- Chubb, C., & Sperling, G. (1988). Drift-balanced random stimuli: a general basis for studying non-Fourier motion perception. *Journal of the Optical Society of America A*, *5*, 1986–2007.
- Field, D. J., Hayes, A., & Hess, R. F. (1993). Contour integration by the human visual system: Evidence for a local “Association Field”. *Vision Research*, *33*, 173–193.
- Graham, N., Sutter, A., & Venkatesan, C. (1993). Spatial-frequency- and orientation-selectivity of simple and complex channels in region segregation. *Vision Research*, *33*, 1893–1911.
- Gray, R., & Regan, D. (1998). Spatial frequency discrimination and detection characteristics for gratings defined by orientation texture. *Vision Research*, *38*, 2601–2617.
- Grossberg, S., & Mingolla, E. (1985). Neural dynamics of perceptual grouping: textures, boundaries, and emergent segmentations. *Perception and Psychophysics*, *38*, 141–171.
- Hubel, D. H., & Wiesel, T. N. (1962). Receptive fields, binocular interaction and functional architecture in the cat’s visual cortex. *The Journal of Physiology*, *160*, 106–154.
- Kingdom, F. A., & Keeble, D. (1996). A linear systems approach to the detection of both abrupt and smooth spatial variations in orientation-defined textures. *Vision Research*, *36*, 409–420.
- Kingdom, F. A., & Keeble, D. (2000). Luminance spatial frequency differences facilitate the segmentation of superimposed textures. *Vision Research*, *40*, 1077–1087.
- Kingdom, F. A., Keeble, D., & Moulden, B. (1995). Sensitivity to orientation modulation in micropattern-based textures. *Vision Research*, *35*, 79–91.
- Knierim, J. J., & Van Essen, D. C. (1992). Neuronal responses to static texture patterns in area V1 of the alert macaque monkey. *Journal of Neurophysiology*, *67*, 961–980.
- Li, C. Y., & Li, W. (1994). Extensive integration field beyond the classical receptive field of cat’s striate cortical neurons—classification and tuning properties. *Vision Research*, *34*, 2337–2355.
- Malik, J., & Perona, P. (1990). Pre-attentive texture discrimination with early visual mechanisms. *Journal of the Optical Society of America A*, *7*, 923–932.
- Mitchison, G., & Crick, F. (1982). Long axons within the striate cortex: their distribution, orientation, and patterns of connection. *Proceedings of the National Academy of Sciences, USA*, *79*, 3661–3665.
- Morgan, M. J., & Hotopf, W. H. N. (1989). Perceived diagonals in grids and lattices. *Vision Research*, *29*, 1005–1015.
- Moulden, B. (1994). Collator units: Second-stage orientational filters. In Higher-order processing in the visual system: Ciba Foundation Symposium 184 (pp. 170–192). Chichester: Wiley.
- Mussap, A. J., & Levi, D. M. (1996). Spatial properties of filters underlying vernier acuity revealed by masking: evidence for collator mechanisms. *Vision Research*, *36*, 2459–2473.
- Mussap, A. J., & Levi, D. M. (1997). Vernier acuity with plaid masks: the role of oriented filters in vernier acuity. *Vision Research*, *37*, 1325–1340.
- Nothdurft, H. C. (1992). Feature analysis and the role of similarity in preattentive vision. *Perception and Psychophysics*, *52*, 355–375.
- Olavarria, J. F., DeYoe, E. A., Knierim, J. J., Fox, J. M., & Van Essen, D. C. (1992). Neuronal responses to visual texture patterns in middle temporal area of the macaque monkey. *Journal of Neurophysiology*, *68*, 164–181.
- Pelli, D. G. (1990). The quantum efficiency of vision. In C. Blakemore (Ed.), *Vision: coding and efficiency* (pp. 1–24). London: Cambridge University Press.
- Pentland, A. (1980). Maximum likelihood estimation: the best PEST. *Perception and Psychophysics*, *28*, 377–379.
- Polat, U., & Sagi, D. (1993). Lateral interactions between spatial channels: suppression and facilitation revealed by lateral masking experiments. *Vision Research*, *33*, 993–999.
- Polat, U., & Sagi, D. (1994). The architecture of perceptual spatial interactions. *Vision Research*, *34*, 73–78.
- Prins, N., & Kingdom, F. A. A. (2002). Orientation- and frequency-modulated textures at low depths of modulation are processed by off-orientation and off-frequency texture mechanisms. *Vision Research*, *42*, 705–713.
- Prins, N., & Mussap, A. J. (2000). Alignment of orientation-modulated textures. *Vision Research*, *40*, 3567–3573.
- Prins, N., & Mussap, A. J. (2001). Adaptation reveals a neural code for the visual location of orientation change. *Perception*, *30*, 669–680.
- Rockland, K. S., & Lund, J. S. (1983). Intrinsic laminar lattice connections in primate visual cortex. *The Journal of Comparative Neurology*, *216*, 303–318.
- Rubenstein, B. S., & Sagi, D. (1993). Effects of foreground scale in texture discrimination tasks: performance is size, shape, and content specific. *Spatial Vision*, *7*, 293–310.

- Schmidt, K. E., Goebel, R., Lowel, S., & Singer, W. (1997). The perceptual grouping criterion of colinearity is reflected by anisotropies of connections in the primary visual cortex. *European Journal of Neuroscience*, *9*, 1083–1089.
- Sillito, A. M., Grieve, K. L., Jones, H. E., Culdeiro, J., & Davis, J. (1995). Visual cortical mechanisms detecting focal orientation discontinuities. *Nature*, *378*, 492–496.
- Smits, J. T. S., Vos, P. G., & van Oeffelen, M. P. (1985). The perception of a dotted line in noise: a model of good continuation and some experimental results. *Spatial Vision*, *1*, 163–177.
- Sutter, A., Beck, J., & Graham, N. (1989). Contrast and spatial variables in texture segregation: Testing a simple spatial-frequency channels model. *Perception and Psychophysics*, *46*, 312–332.
- Sutter, A., Sperling, G., & Chubb, C. (1995). Measuring the spatial frequency selectivity of second-order texture mechanisms. *Vision Research*, *35*, 915–924.
- Tripathy, S. P., Mussap, A. J., & Barlow, H. B. (1999). Detecting collinear dots in noise. *Vision Research*, *39*, 4161–4171.
- von der Heydt, R., Peterhans, E., & Dürsteler, M. R. (1992). Periodic-pattern-selective cells in monkey visual cortex. *Journal of Neuroscience*, *12*, 1416–1434.
- Zhou, Y. X., & Baker, C. L. (1993). A processing stream in mammalian visual cortex neurons for non-Fourier responses. *Science*, *261*, 98–101.
- Zipser, K., Lamme, A. F., & Schiller, P. H. (1996). Contextual modulation in primary visual cortex. *The Journal of Neuroscience*, *16*, 7376–7389.